



HAL
open science

Advanced system-level simulation paradigm for ultra-wideband systems using SCERNE platform

Mohammad Ojaroudi, Stéphane Bila, Edouard Ngoya, Sébastien Mons, François Torres, Arnaud Beaumont, Julien Lintignat

► To cite this version:

Mohammad Ojaroudi, Stéphane Bila, Edouard Ngoya, Sébastien Mons, François Torres, et al.. Advanced system-level simulation paradigm for ultra-wideband systems using SCERNE platform. *International Journal of RF and Microwave Computer-Aided Engineering*, 2019, 29 (12), 10.1002/mmce.21975 . hal-02353119

HAL Id: hal-02353119

<https://unilim.hal.science/hal-02353119>

Submitted on 9 Dec 2020

HAL is a multi-disciplinary open access archive for the deposit and dissemination of scientific research documents, whether they are published or not. The documents may come from teaching and research institutions in France or abroad, or from public or private research centers.

L'archive ouverte pluridisciplinaire **HAL**, est destinée au dépôt et à la diffusion de documents scientifiques de niveau recherche, publiés ou non, émanant des établissements d'enseignement et de recherche français ou étrangers, des laboratoires publics ou privés.

Advanced System Level Simulation Paradigm for UWB Systems using SCERNE Platform

M. Ojaroudi, S. Bila, E. Ngoya, S. Mons, F. Torrès, A. Beaumont and J. Lintigant

XLIM, UMR 7252, University of Limoges/CNRS, 123 Av. Albert Thomas, 87060 Limoges, France

Abstract—In this paper, a progressive system level simulation framework is developed based on SCERNE platform to simulate an UWB impulse radar transmitter and accurately predict its performance. With the purpose of demonstrating the usefulness of the SCERNE ability in system level modeling, we present and simulate a simplified structure of UWB impulse radar transmitter. First, after simulation each component in different circuit-level tools such as ADS, CST and HFSS, each part has been modeled by using different modeling methods to transfer their data into MATLAB environment. Then, we duplicate the transmitter structure in SCERNE toolbox to validate the results. The advantage conferred by the proposed SCERNE toolbox is that fast and accurate bilateral modeling method is available at multi-medium structures in contrast with conventional unilateral modeling, and so a lower memory and higher accuracy of the behavioral model is achieved. It can also be beneficial when the user is looking for system-level, as the increased components amounts can help as a surrogate model. The system model can be easily extended to other UWB radar systems by simply changing the input pulse shape, UWB channel environment, transceiver topology, etc. Various effects such as signal quality, and pulse shape that can easily investigate and re-optimize for high performance are using the developed model. To validate the practicality of the proposed paradigm, the simulations and predictions through model results are being outlined.

Index Terms—SCERNE ("Simulation de Chaînes d'Emission/Réception Nouvelle gEnération"), Ultra-Wideband Impulse Radar (UWB-IR), Step-Recovery Diode (SRD), Artificial Neural Network (ANN), Polynomial Rational Functions.

1. Introduction

A challenging obstacle in system-level multi-parameter modeling and optimization is the interdependence of the parameters of the device being designed due to designing in multi-mediums criteria. Typically, in order to design an UWB transceiver, different software in multi-medium framework are needed. Designing of each component is done in a special software using different modeling methods are based on different parameters [1-2]. However, sometimes it is impractical to find good intercommunication among all of the parameters, especially in UWB systems (because of the large number of frequency samples needed to fit the bandwidth). One of the main examples of multi-parameter design process is UWB impulse radar transmitter, connecting both active and passive components within a wide frequency range. In order to solve this obstacle, a few methods for multi-criterion design optimization of UWB impulse radar transmitter's components have recently been presented and evaluated in the literature [3-4].

SCERNE is a platform for the modeling and simulation of RF front end at system-level [5]. The generalist programmable environment called SCERNE ("Simulation de Chaînes d'Emission/Réception Nouvelle gEnération") in french, which may be translated as "New Generation Simulation of Emission/Reception Chains") integrates these elements and thus facilitates the development and the validation of new models which will be added to SCERNE's palette. This enables the models to be integrated into generalist, multi-domain and heterogeneous system simulators. In this platform several optimization algorithms and tools for mathematical analysis are also developed alongside. Information about structure is an essential requirement for the operation of modeling. In this point of view, extracted models can be incorporated into SCERNE as component models for fast and accurate system-level simulation and optimization [5-6]. The extracted EM data from EM simulator (e.g., CST [7], ADS [8], and HFSS [9]) are used to extract head files in SCERNE. The extracted files are then incorporated into a system-level simulator. It enables fast simulation and optimization of an RF front-end system using the component, e.g., in this study a pulse generator, a low-

pass filter, a monopole antenna for UWB frequency range, as an impulse radar transmitter. Whereas the model is parametric, without having to remodel the original EM simulation, the physical parameters of this component is adjustable during the circuit simulation, optimization, and statistical design. In addition, the models are developed only once and then can be reused for many different circuit optimizations [6].

In this paper, with the purpose of system-level modeling of the UWB-IR transmitter, SCIENCE framework is being used as a consecutive model of pulse generator, low-pass filter and UWB antenna. Owing to SCERNE, it is the first time a novel type of bilateral blocks modeling has been applied for simultaneously calculating scattering and propagation parameters of an impulse radar's transmitter amongst the system-level models for RF front-end structure reported lately [10]. A comparison between simulated results using EM simulators and values predicted from extracted models is shown to validate the effectiveness of the SCERNE framework for precisely calculating the time domain transmitted pulse. Comparison results demonstrate that SCERNE toolbox could be an acceptable candidate for advanced multi-medium system level simulation.

2. UWB impulse radar transmitter Design and Configuration

The detailed block diagram of the simulated UWB impulse radar's transmitter is presented in Figure 1. In this study, at the transmitting link, a step recovery diode based pulse generator is designed to produce a sub-nanosecond pulse. The generated pulse is modulated by a 4 GHz carrier signal through a mixer before passing through a low pass filter and a high gain power amplifier. The amplified signal is then sent out through a designed UWB antenna. After separately modeling and simulating each component, we introduce SCERNE as a multi-medium modeling toolbox to support all modeled components. Since SCERNE is based on MATLAB-Simulink, it covers all types of MATLAB-based optimization techniques like Artificial Neural Network (ANN), Genetic Algorithm (GA), etc. It also supports multiple representing and modeling techniques like steady state, pole-residue transfer function, etc. Figure 2 shows the proposed advanced system level co-design for UWB systems using SCERNE toolbox.

A. UWB SRD Based Pulse Generator Modeling

With the intention of designing and modeling an UWB-IR transmitter, the design of an UWB pulse generator is the first step. Figure 3 demonstrated the simulated SRD-based UWB pulse generator circuit in ADS software based on pulse-shaping technique using $\lambda/4$ short circuit microstrip line. As shown in Figure 3 for the applied case, an input-matching network is developed in order to eliminate pulse distortion [11]. The matching network is an R-C low-pass filter, which allows only the triggering signal (in this study its frequency is 10 MHz) to pass and bypasses the leaked fast step signal.

In addition, the equivalent circuit of the proposed SRD-based pulse generator with matching circuits components (C_1 and L) is shown in Fig 4. SRD can be treated equivalently as a small resistance (R_0) and a large capacitance (C_0) when the forward direction is conducting and its on-state voltage is more than 0.5V. The on-state equivalent circuit is shown in Figure 4 (a). In the case of the SRD conversion from the forward to the backward bias, SRD is still on at a voltage of about 0.3V and the current is in the reverse direction before the SRD junction charge is depleted [12]. In addition, SRD can be equivalently seen as a variable capacitance (C_d) at reverse cut-off, and the equivalent circuit is shown in Figure 4 (b). The time domain response of the circuit during the SRD cut-off can be analyzed using the Kirchhoff theorem. The voltages at both sides of SRD are the on-state voltages, when SRD is on and stable. We can consider that the capacitance value C_d is fixed. According to the Kirchhoff theorem, the second-order differential equation of the voltage V_0 at both sides of SRD can be written as follows:

$$\frac{C_1 C_d}{C_1 + C_d} \frac{d^2 V_0}{dt^2} + \frac{dV_0}{R dt} + \frac{V_0}{L} = 0 \quad (1)$$

Regarding the infinitesimal analysis principles, V_0 can be calculated using equation (1) when the values of C_d , L , C_1 and R are known as equation (2):

$$V_0(t) = \frac{-\frac{c_1 + c_d}{c_1 c_d} \left(I_L(0) + \frac{V_0(0)}{R} \right) - V_0(0) x_2}{x_1 - x_2} e^{x_1(t)} + \frac{-\frac{c_1 + c_d}{c_1 c_d} \left(I_L(0) + \frac{V_0(0)}{R} \right) - V_0(0) x_1}{x_2 - x_1} e^{x_2(t)} \quad (2)$$

$$\text{Where } x_1 = \frac{-\frac{c_1 + c_d}{c_1 c_d R} + \sqrt{\left(\frac{c_1 + c_d}{c_1 c_d R}\right)^2 - 4 \frac{c_1 + c_d}{c_1 c_d L}}}{2}, \quad x_2 = \frac{-\frac{c_1 + c_d}{c_1 c_d R} - \sqrt{\left(\frac{c_1 + c_d}{c_1 c_d R}\right)^2 - 4 \frac{c_1 + c_d}{c_1 c_d L}}}{2}$$

It is obvious from the equation (2), that the width, amplitude and shape of the generated pulse are extremely dependent on the exciting inductance L and C_d . When other parameters are given, a small value of L means that the pulse width is narrow, the amplitude is small, and the pulse ringing is serious. In addition, a small value of C_d causes a narrow pulse width, larger amplitude, and slight pulse ringing. Therefore, the SRD with small junction capacitance (C_d) is recommended for the circuit design, and the value of L should be chosen taking pulse width and amplitude into account. In this study, based on equation (2) for suitable fitting of ADS result, the generated signal has been modeled like double exponential pulse waveform as follows [13]:

$$V_0(t) = A e^{-\alpha(t)} - B e^{-\beta(t)} \quad (3)$$

where $A=35$ and $B=5$ are the amplitudes, $\alpha=3.5 \times 10^9 \text{ sec}^{-1}$ and $\beta=4.5 \times 10^9 \text{ sec}^{-1}$ and t is the time in seconds. The use of this waveform was motivated by the fact that it provides the closest functional fit to the type of pulse shapes that could be generated experimentally by SRD based pulse generator. Figure 5 depicts both the ADS simulation and modeled results. As shown in Figure 5, in the simulated case, the pulse width is much wider and has severe distortion.

B. Modeling of the Low Pass Filter using Polynomial Rational Function

Herein, low-pass filter is considered as the second component in UWB-IR transmitter circuit. For this section, we proposed a low pass filter using defected ground structure (DGS) slots and T-shaped arms as shown in Figure 6. The proposed DGS slot is shown in Figure 6 (b). The etched defect in the ground plane disturbs the shield current distribution in the ground plane. This disturbance can increase the effective capacitance and inductance of a transmission line. Thus, an LC equivalent circuit can represent the proposed unit DGS circuit [14]. The resonant frequency of the slot can be modified by changing the overall slot size and the distance between the folded T-shaped arms, which shifts the cutoff frequency of the filter down. A parametric study, shown in Figure 7, was carried out to show the effect of the slots length on the resonant frequency, particularly on the resonance of the parallel resonator, which represents two transmission zeroes. The final values of the presented band-stop filter design parameters are specified in Table 1.

After collecting EM data of the proposed filter depending on different geometrical/physical parameters from CST simulation we can represent an equivalent circuit. For a given frequency range, we can use transfer functions (polynomial rational functions) to represent the electrical behavior (e.g., ABCD matrix) of the proposed filter. For any two-port embedded passives, the following scattering functions are adequate to represent S_{11} and S_{21} respectively [15].

$$S_{11} = \frac{b_0 + b_1 s + \dots + b_{n-1} s^{n-1} + b_n s^n}{a_0 + a_1 s + \dots + a_{n-1} s^{n-1} + a_n s^n} \quad (4)$$

$$S_{21} = \frac{d_0 + d_1 s + \dots + d_{n-1} s^{n-1} + d_n s^n}{c + c_1 s + \dots + c_{n-1} s^{n-1} + c_n s^n} \quad (5)$$

where $s = j\omega$, and n is the effective order of the polynomial. In order to capture a more accurate assessment for the scattering characteristics of the proposed low pass microstrip filter, we use a high-order equivalent circuit model as shown in Figure 8. Specifically, a cascade form of parallel resonance circuits is used to demonstrate the frequency characteristics of the defected ground structure (DGS) more clearly [15]. Figure 9 shows the modeled return and insertion loss of the filter in comparison with simulated results from CST. Two transmission zeroes, which improves behavior of the filter stop band, is observed at 10.8 GHz and 11.6 GHz.

C. Multi-Parameters Modeling of the UWB Antenna Based on Neural Network

The last component that will be modeled in the proposed transmitter is an antenna. The UWB microstrip monopole antenna depicts in Figure 10 that is being used in our modeling [17]. It is printed on a 1.6 mm-thick FR4 substrate (dielectric constant of 4.3). Regarding defected-ground structure (DGS), creating a pair of protruded rectangular ring strips in the ground plane's corners like ground plane's sleeve provides an additional current path [16]. In addition, by inserting circular shaped tapered strip of convenient dimensions between the patch and microstrip feed-line, a wide-band feeding structure can be produced. In the proposed design, the excitation of horizontal currents is prevented by insertion of symmetric wide structures in feed [17]. As a result, an improvement in the impedance bandwidth and gain properties of the monopole is achieved. The modified design parameters of the UWB antenna are summarized in Table II.

In order to develop a compact neural network model, input and output variables of the monopole antenna are defined. First, we generate physics-based input-output simulation data using HFSS software. In the abovementioned parametric sweep simulation, some physical parameters such as widths and lengths of the slots and sleeves have been defined as input variables and the electrical parameters of the antenna such as return loss and maximum gain are defined as output variables. In the next step, the generated data, i.e., training data, are used to train the neural network model. The representation of the monopole antenna by neural network is shown in Figure 11. As shown in Figure 11, W_s , L_s and W_d are input variables and S_{11} and maximum gain are the outputs of the trained model.

In this study, a multi-layer perceptron (MLP) neural network fed by CST output is trained to approximate S_{11} and maximum gain parameters in the frequency of interest. MLP neural network can be used to develop new models or to enhance the accuracy of existing models. They learn device data through an automated training process, and the trained neural networks are then used as fast and accurate models for efficient high-level circuit and system design. These models have the ability to capture multidimensional arbitrary nonlinear relationships. The theoretical basis of neural networks is based on the universal approximation theory [18], which states that a neural network with at least one hidden layer can approximate any nonlinear continuous multidimensional function to any desired accuracy. This makes neural networks a useful choice for multi-parameter modeling where a mathematical model is not available and the relationship between parameters are unknown. As illustrated in Figure 11, a multilayer perceptron network consists of an input layer, one or more hidden layers, and an output layer [18]. In the MLP network, each neuron processes the inputs received from other neurons or from the network inputs.

Based on the above discussion, we present in this section the proposed MLP neural network modeling to build high accuracy multi-parameters model, and in the next section we will show some simulation results. The hidden and output layer transfer functions are hyperbolic tangent sigmoid and linear functions, respectively. Sixty input vectors x , are used as training patterns. In this study, the input data is divided into three sets, randomly, as: 60% for training, 20% for validation, and 20% for performance test. The training algorithm is performed using the Levenberg-Marquardt method. The training data are used to train the MLP, while the validation data will be used to check the performance of the model. Proper distribution of the data is controlled by simultaneously checking the plots of test and validation errors [19]. The learning rate, maximum number of epoch, and maximum mean square error are set to 0.05, 1000, 0.001, respectively. Table III shows the trained MLP characteristics.

The proposed antenna with optimal design is simulated in the HFSS simulator and the return loss, and maximum gain characteristics of the proposed antenna are compared with predicted results from neural network model. Figures 12 and 13 compare the return loss and maximum gain characteristics of the antenna computed using HFSS and the trained ANN, respectively. As shown in these figures, there is good accuracy between neural network model outputs and simulated data. As shown in Figures 12 and 13, there exists a discrepancy between predicted data and the simulated results. This discrepancy is mostly due to the number of input parameters. In this study, the input parameters of the neural network are W_s , L_s and W_d and others are fixed. In order to confirm the accuracy of return loss and gain characteristics for the designed antenna, it is recommended that more parameters used as input of the neural network.

3. Advanced System Level Simulation in SCERNE

In order to illustrate effectiveness of SCERNE platform on multi-parameter system level simulation first, head files in SCERNE are extracted. Figure 14, 15 and 16 show simulated and extracted signals of three simulated and modeled components of the proposed UWB-IR transmitter.

In the next step, the proposed transmitter including modulated pulse generator, low pass filter and an antenna is simulated in SCERNE as shown in Figure 17. Unlike other system-level simulators like Agilent Ptolemy that has unilateral blocks, SCERNE handles unilateral as well as bilateral blocks, the same way as circuit level simulators. By using these blocks, we will have forward and backward signal paths. Figure 18 shows incident waves to the input and the load of the cascade connection of the pulse generator, filter and antenna in different scenarios. As shown in Figure 18 (a) after adding the filter to the pulse generator with modulator it causes a slight drop in signal amplitude because of the filter insertion loss. Figure 18 (b) shows the effect of adding the antenna on the pulse amplitude, which is generated in previous state without antenna. From Figure 18 (b) it can be concluded that adding antenna decreases the amplitude of the generated pulse up to half of the pulse amplitude. This decrease due to, is because of bilateral blocks effect. In other words, antenna can be operated as an open circuit and the reflected signal will decrease the generated pulse at the pulse generator output.

Figure 19 shows the proposed transmitter simulated in Agilent Ptolemy. In addition, a comparison of the output signal for the simulated transmitters in Agilent Ptolemy and SCERNE is shown in Figure 20. The predicted results show good agreement with simulation results and demonstrate that excellent reflected signal effects could be by using bi-lateral blocks performance in SCERNE.

4. Conclusion

In this paper, a new approach of high-accuracy multi-medium modeling of an UWB impulse radar transmitter using SCERNE platform is presented. First, after using different software to design optimal components, we extracted models of each component based on different modeling techniques. Then, in order to show SCERNE effectiveness in system-level multi-medium modeling a hierarchical structure of pulse generator, filter and an antenna is simulated in SCERNE environment. The simulated results confirmed that the predicted results from models are fairly close to SCERNE results. Therefore, the extracted and simulated output in SCERNE can be used instead of different software results. Under the default option, the extracted model in SCERNE is several times faster than the simulated model in CST, HFSS and ADS. This helps the designer to have a fast and accurate surrogate model with the ability to design multi-mediums structure while having multi-parameters design flow.

References

- [1] Wang, Y. and Fathy, A.E., Advanced system level simulation platform for three-dimensional UWB through-wall imaging SAR using time-domain approach. *IEEE Transactions on Geoscience and Remote Sensing*, 50(5), pp.1986-2000, 2012.
- [2] A. Costanzo, D. Masotti, M. Fantuzzi and M. Del Prete, "Co-Design Strategies for Energy-Efficient UWB and UHF Wireless Systems," in *IEEE Transactions on Microwave Theory and Techniques*, vol. 65, no. 5, pp. 1852-1863, May 2017.
- [3] Z. Yang and K. F. Warnick, "Analysis and Design of Intrinsically Dual Circular Polarized Microstrip Antennas Using an Equivalent Circuit Model and Jones Matrix Formulation," in *IEEE Transactions on Antennas and Propagation*, vol. 64, no. 9, pp. 3858-3868, Sept. 2016.
- [4] A. Bennadji, A. Soury, E. Ngoya, *et al.* Implementation of behavioral models in system simulator and rf circuit/system co-simulation. In : *Integrated Nonlinear Microwave and Millimeter-Wave Circuits, 2006 International Workshop on*. IEEE, 2006. p. 168-171.
- [5] Mons, S., Ngoya, E., Quere, R., Layec, A., Dallet, D., Lacombe, P., Mazeau, J., Decaesteke, T., Martinaud, J.P., Phelion, O. and Reptin, F., 2011, April. SCERNE, an efficient CAD tool for the modeling of RF and Mixed blocks. In *Integrated Nonlinear Microwave and Millimeter-Wave Circuits (INMMIC), 2011 Workshop on* (pp. 1-4). IEEE.
- [6] REVEYRAND, Tibault, BARATAUD, Denis, NEVEUX, Guillaume, *et al.* Overview on system level simulation environment for characterization, modeling and simulation of RF and microwave devices. In : *Integrated Nonlinear Microwave and Millimeter-Wave Circuits, 2006 International Workshop on*. IEEE, 2006. p. 128-131.
- [7] CST Microwave Studio. ver. 2014, CST, Framingham, MA, USA, 2014.
- [8] Advanced Design System (ADS), Agilent Corporation, 2015.
- [9] Ansoft High Frequency Structure Simulation (HFSS), Ver. 13, Ansoft Corporation, 2013.
- [10] A. Bennadji, and all., "Modeling of a communication chain with implementation of a Volterra power amplifier model for efficient system level simulation", European Conference on Wireless Technology, 2005, pp. 101-104.
- [11] C. Zhang, and A. E. Fathy, Reconfigurable pico-pulse generator for UWB applications. In : *Microwave Symposium Digest, 2006. IEEE MTT-S International*. IEEE, 2006. p. 407-410.

- [12] L. Zou, , Sh. Gupta, et Ch. Caloz, A simple picosecond pulse generator based on a pair of step recovery diodes. *IEEE Microwave and Wireless Components Letters*, 2017.
- [13] M Ojaroudi, E. Mehrshahi, and A. Fathy, "A novel approach of modified excitation signal using an UWB pulse generator for high-resolution applications," *Microwave and Optical Technology Letters*, vol. 56, no. 12, pp. 2987-2990, 2014.
- [14] W. Menzel, et A. Balalem, Compact suspended stripline quasi-elliptic low-pass filters. In : *German Microwave Conf.* 2005. p. 61-64.
- [15] Xu, L.J. and Duan, Z., 2017. Miniaturized lowpass filter with wide band rejection using modified stepped-impedance hairpin resonator. *Microwave and Optical Technology Letters*, 59(6), pp.1313-1317.
- [16] Wu, J.W., Hsieh, D.H., Cheng, Y.W., Wang, W.T. and Wang, C.J., 2015, January. Small low-pass filter using slotted-ground-plane resonator. In *Radio and Wireless Symposium (RWS), 2015 IEEE* (pp. 144-146).
- [17] M. Ojaroudi, S. Bila, F. Torrès, "A New Approach of Multi-Parameter UWB Antenna Modeling Based on Knowledge-Based Artificial Neural Network", Accepted to Publish in *12th European Conference on Antennas and Propagation (EUCAP)*, 9-13 April , London, 2018.
- [18] Q. J. Zhang and K. C. Gupta, *Neural Networks for RF and Microwave Design*. Boston: Artech House, 2000
- [19] H. Kabir, L. Zhang, M. Yu, P. H. Aaen, J. Wood and Q. J. Zhang, "Smart Modeling of Microwave Devices," in *IEEE Microwave Magazine*, vol. 11, no. 3, pp. 105-118, May 2010.

Figure Captions:

- Figure 1. Detailed diagram of the simulated UWB impulse radar transmitter.
- Figure 2. The proposed advanced system level co-design for UWB systems using SCERNE toolbox.
- Figure 3. Simulated SRD-based UWB pulse generator circuit in ADS software.
- Figure 4. Equivalent circuits of the proposed SRD-based UWB pulse generator during (a) conduction (b) cut-off.
- Figure 5. Simulated and modeled of the generated signal of the proposed SRD based pulse generator.
- Figure 6. The proposed low-pass microstrip schematic, (a) top layer, and (b) bottom layer.
- Figure 7. Insertion/return loss of the proposed low-pass filter based on parametric sweep of L_{p3} from 0 to 2 mm in CST.
- Figure 8. Extracted the equivalent circuit model for the proposed low-pass filter in ADS.
- Figure 9. Simulated and modeled return/insertion loss of the proposed filter.
- Figure 10. Geometry of the proposed sleeve monopole antenna with circular-tapered feed-line [17].
- Figure 11. Representation of the proposed antenna by a surrogate neural network model.
- Figure 12. Comparison of return loss characteristics of the proposed antenna evaluated from the neural network model versus EM simulation from HFSS [17].
- Figure 13. Comparison of the maximum gain of the proposed antenna evaluated from the neural network model versus EM simulation from HFSS [17].
- Figure 14. Extracted generated signal of the proposed modulated pulse generator from ADS to SCERNE.
- Figure 15. Extracted S-parameter of the proposed filter from CST to SCERNE.
- Figure 16. Extracted S-parameter of the proposed antenna from HFSS to SCERNE.
- Figure 17. The proposed transmitter simulated in SCERNE.
- Figure 18. Comparing single pulse generator signal (V_{in}) with transmitter output signal (V_{out}), (a) after adding filter, and (b) after adding filter and antenna.
- Figure 19. The proposed transmitter simulated in the Agilent Ptolemy (ADS).
- Figure 20. Comparison of the output signal for the simulated transmitters in Agilent Ptolemy (ADS) and SCERNE.

Table Captions:

TABLE I: The proposed Low-Pass Filter dimensions

TABLE II: The proposed monopole antenna dimensions

TABLE III: The trained MLP characteristics

Figure. 1

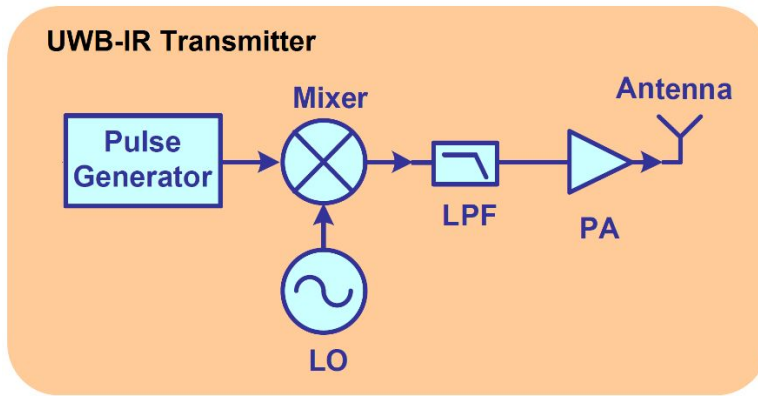


Figure. 2

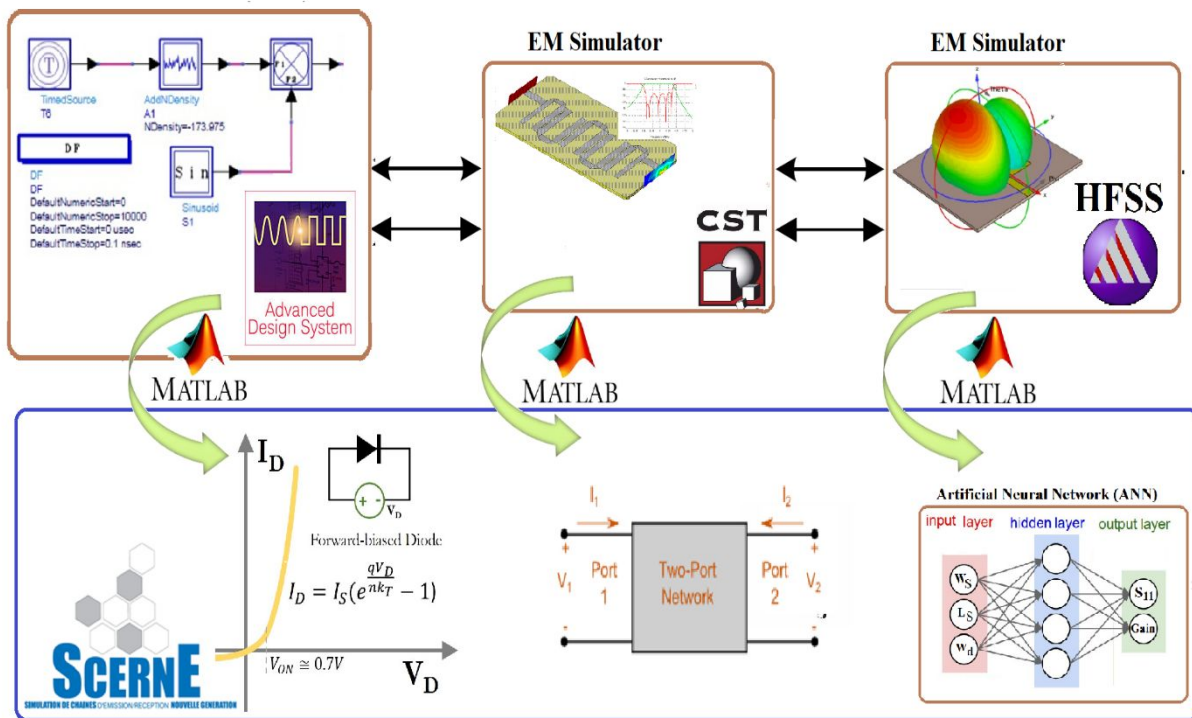


Figure. 3

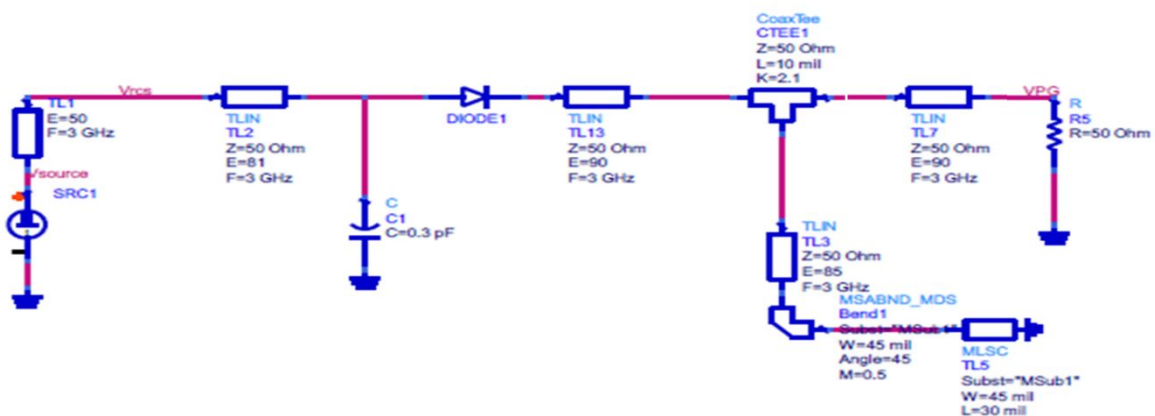


Figure. 4

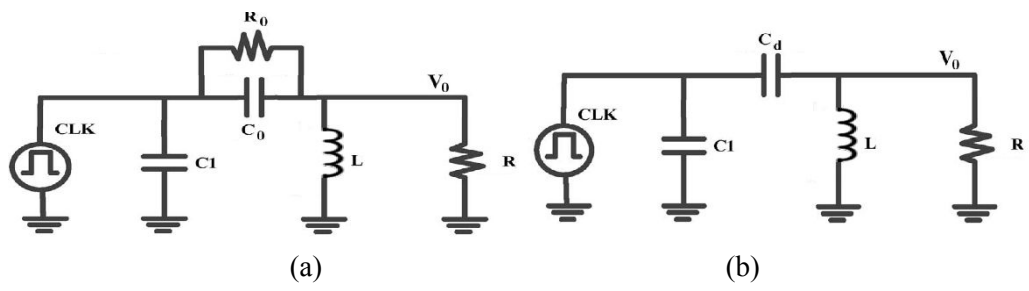


Figure. 5

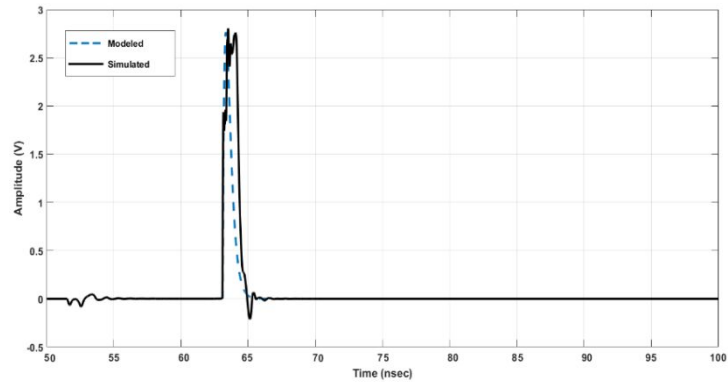
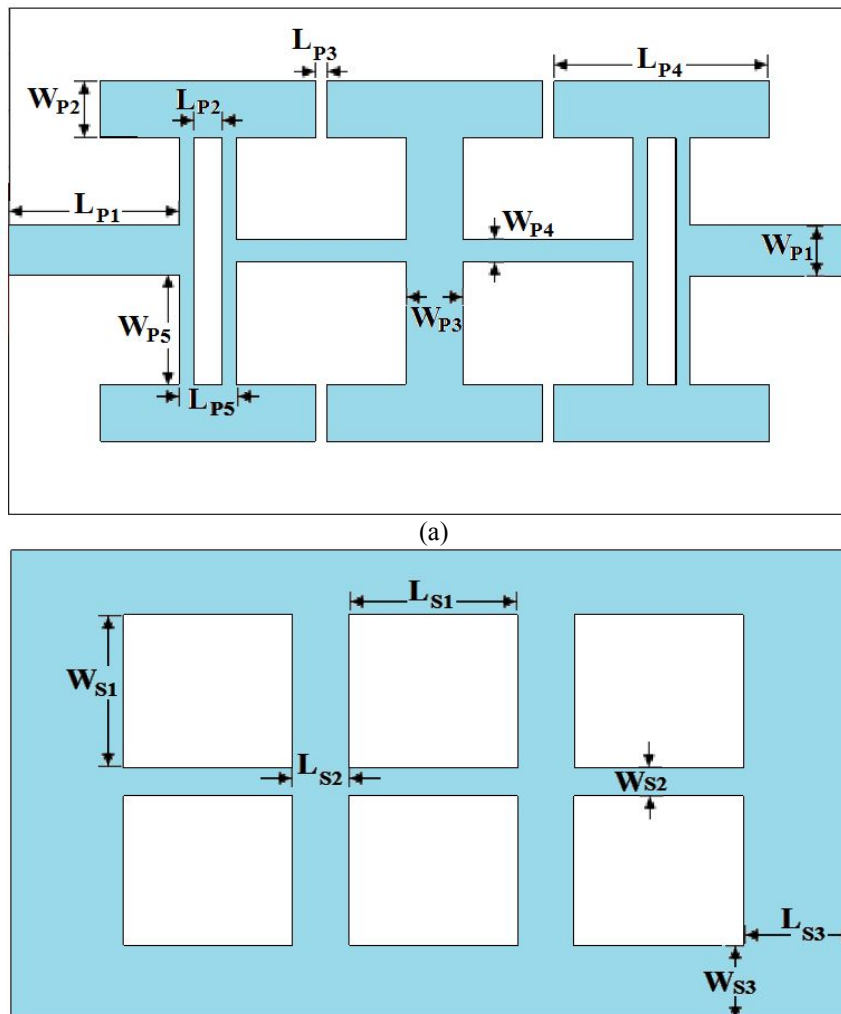


Figure. 6



(b)

Figure. 7

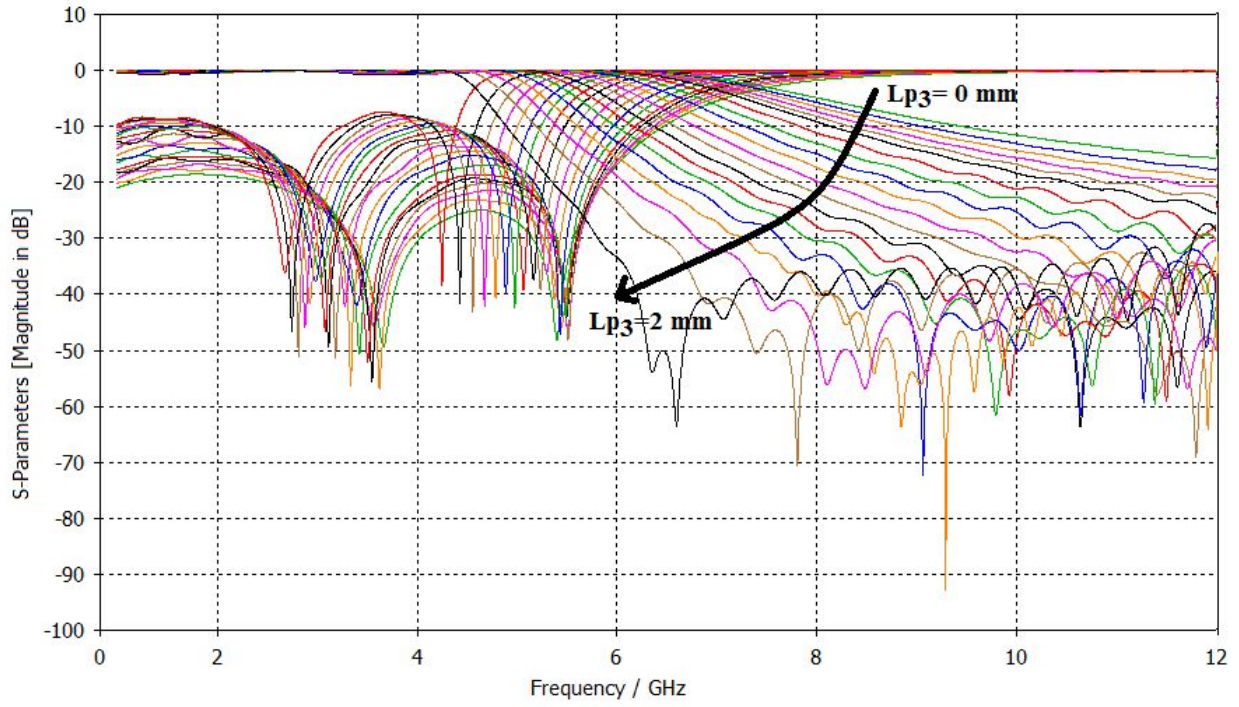


Figure. 8

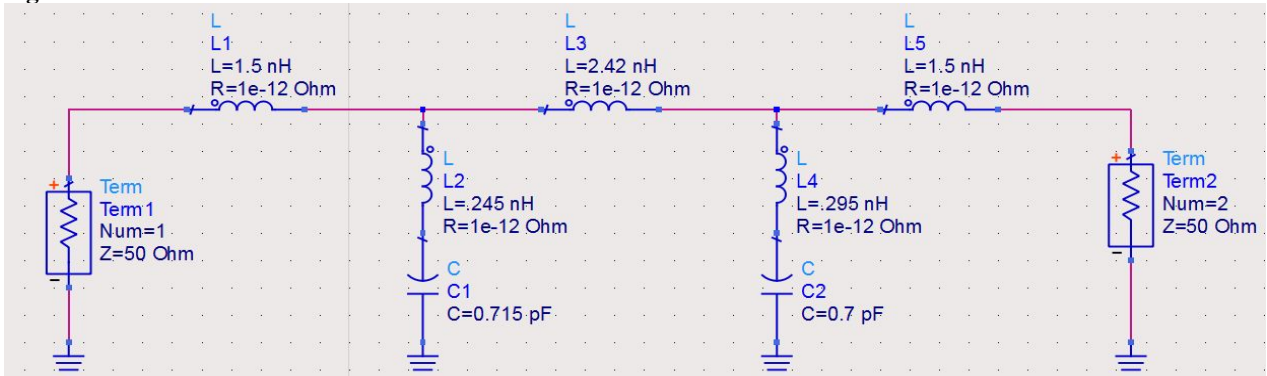


Figure. 9

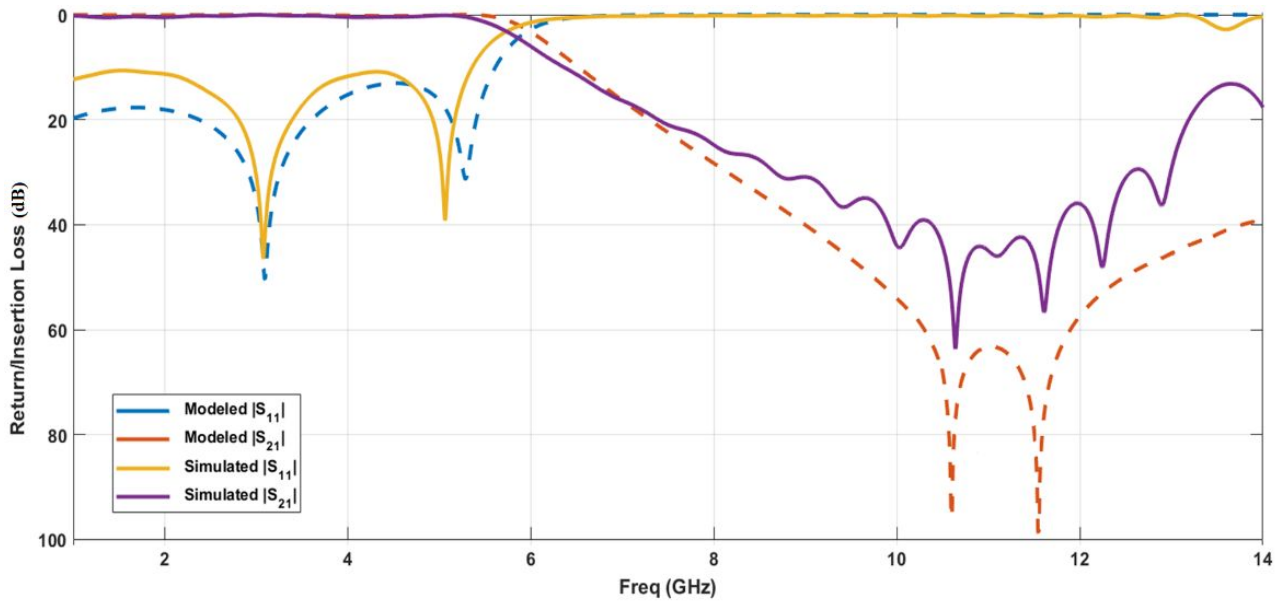


Figure. 10

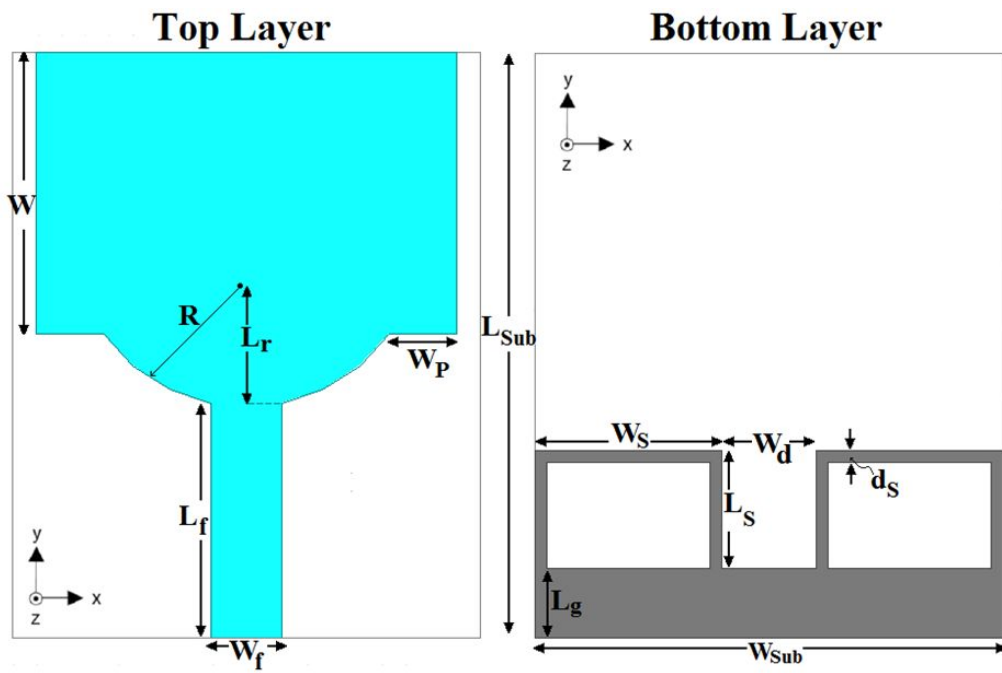


Figure. 11

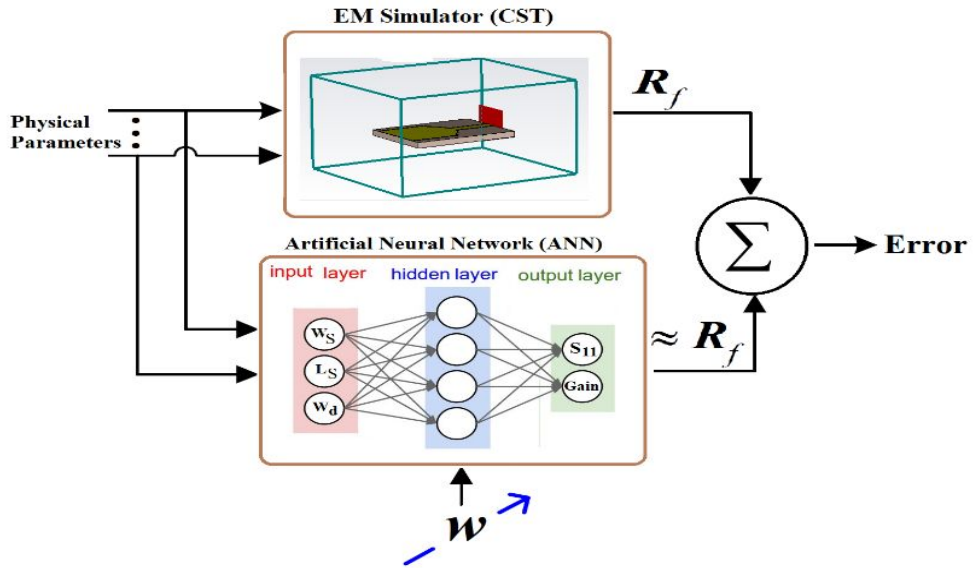


Figure. 12

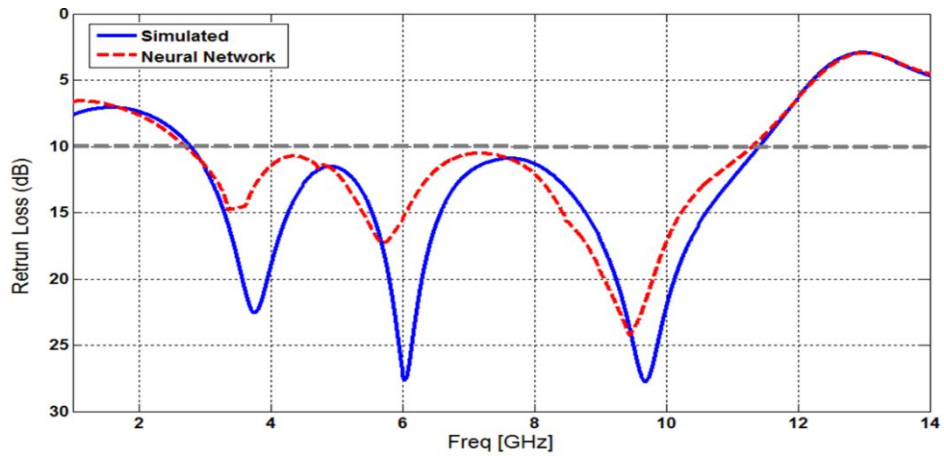


Figure. 13

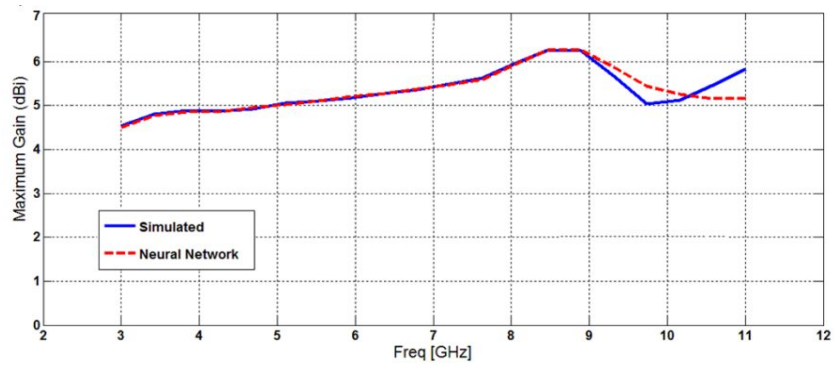


Figure. 14

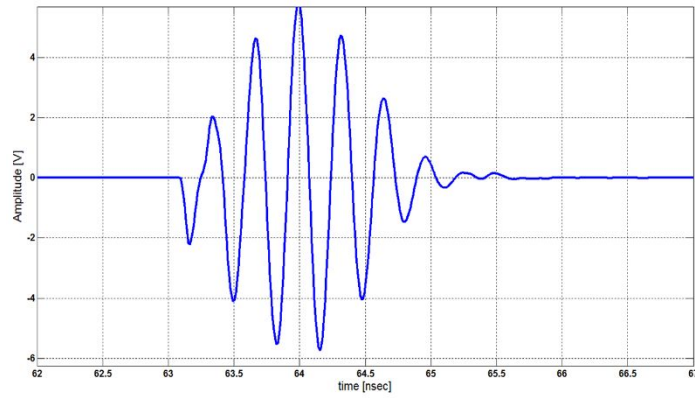


Figure. 15

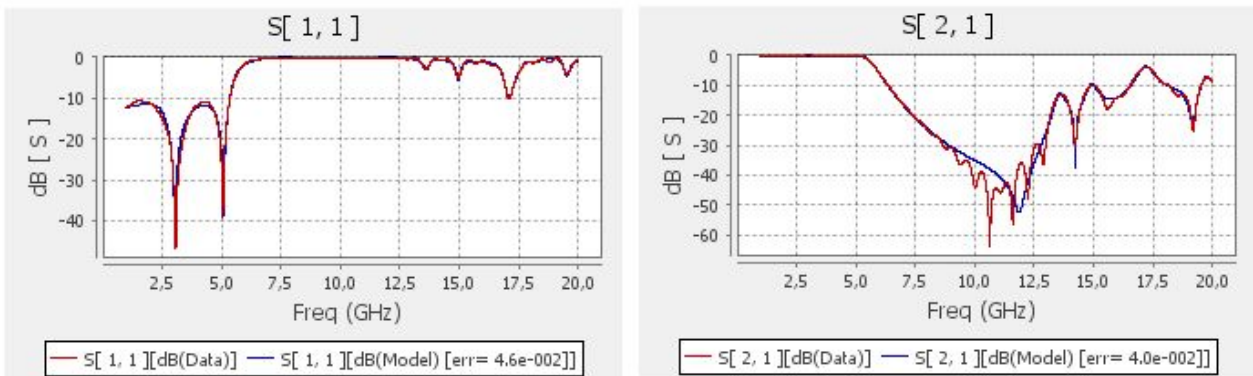


Figure. 16

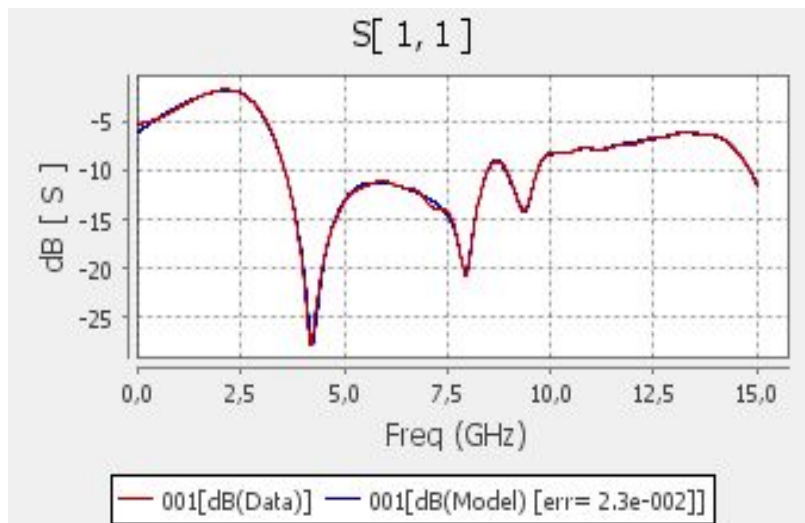


Figure. 17

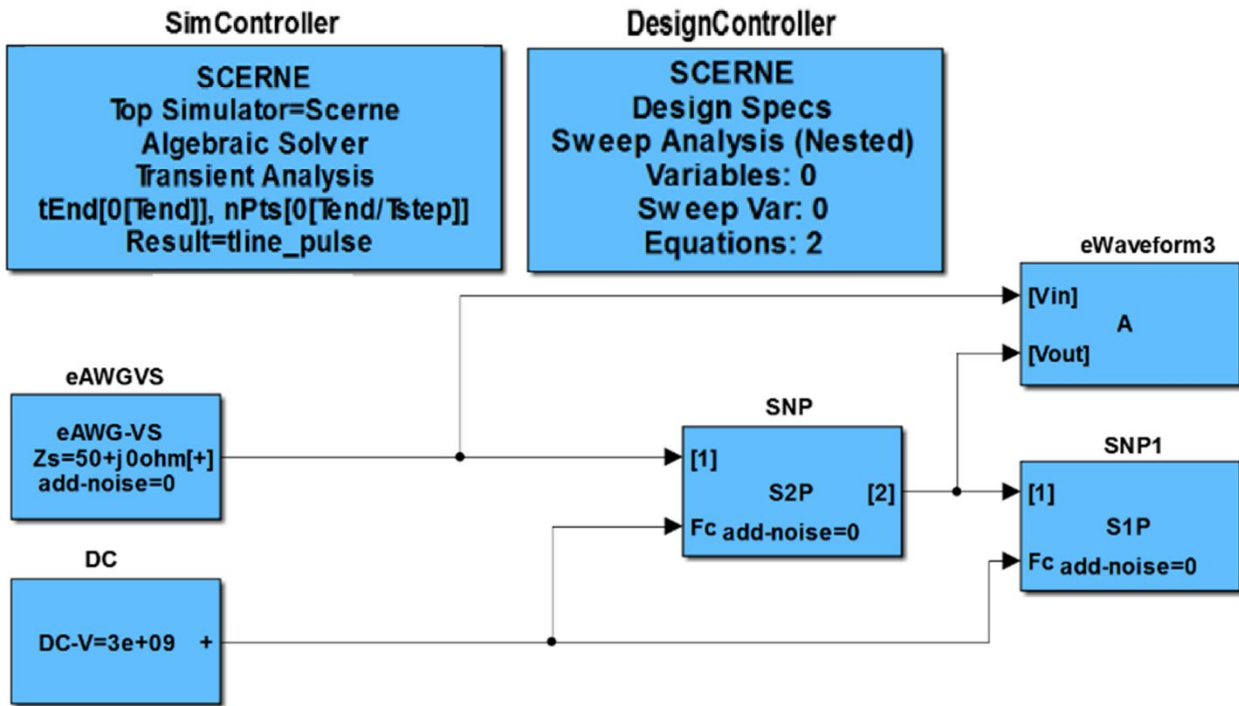


Figure. 18

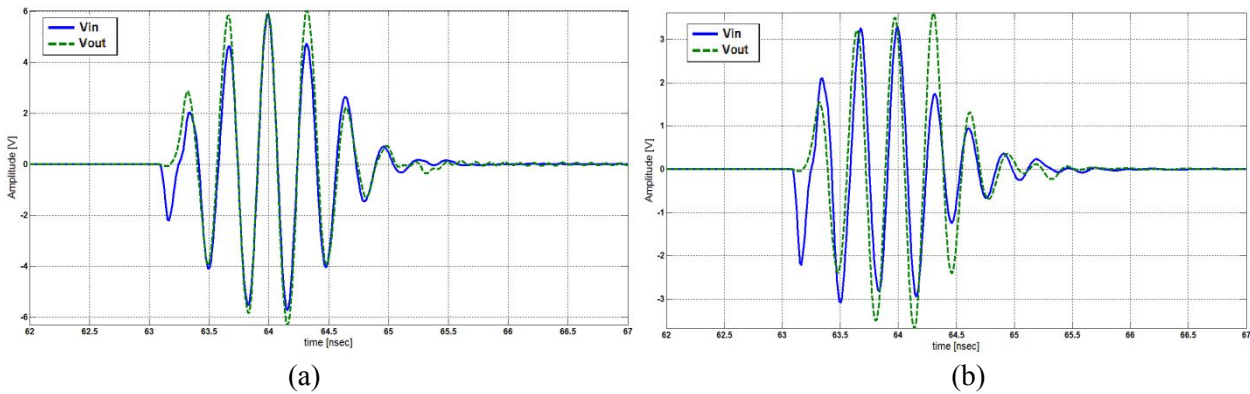


Figure. 19

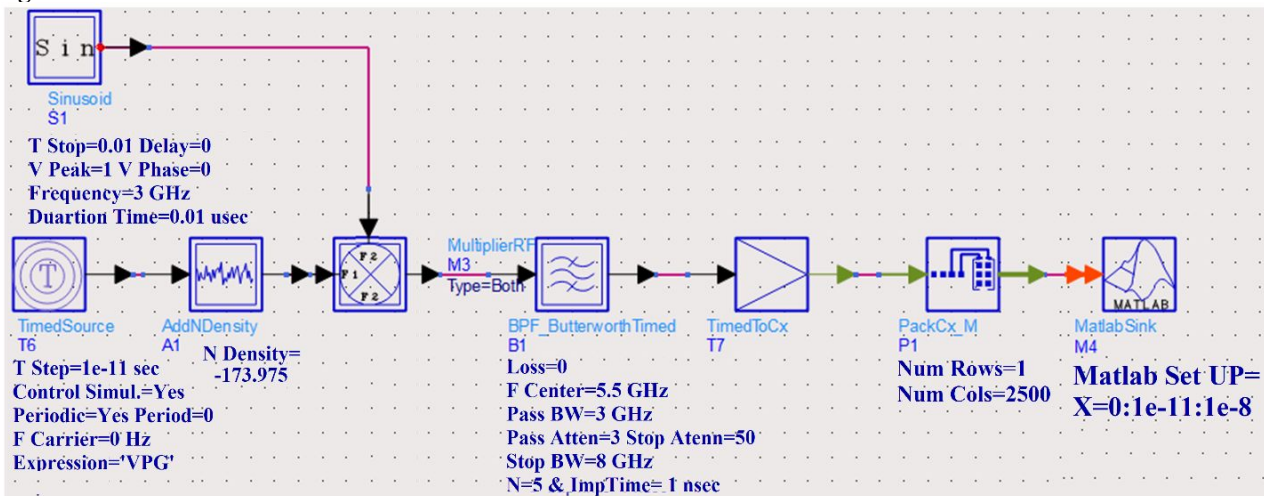


Figure. 20

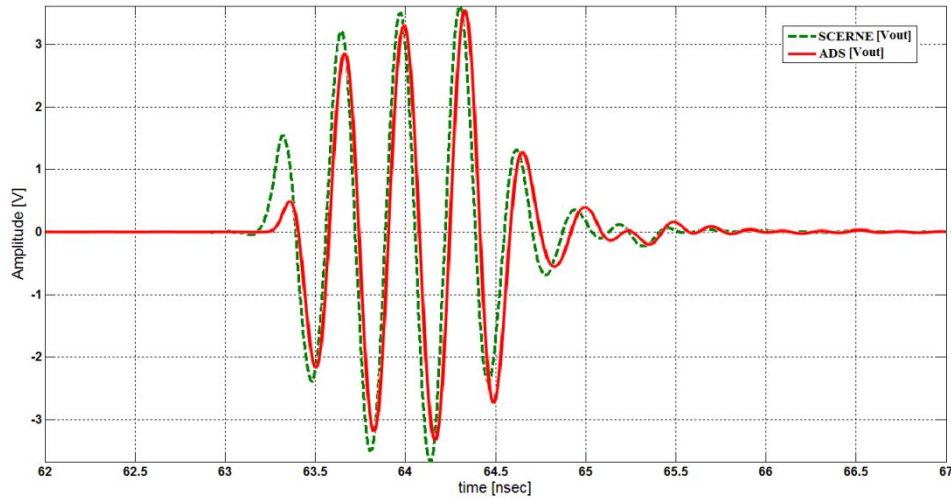


TABLE I.

Parameter	Value(mm)	Parameter	Value(mm)
W_{P1}	0.9	L_{P1}	3
W_{P2}	1	L_{P2}	0.5
W_{P3}	1	L_{P3}	0.2
W_{P4}	0.4	L_{P4}	3.8
W_{S3}	1.5	L_{S3}	2
W_{S2}	0.5	L_{S2}	1
W_{S1}	3.25	L_{S1}	3

TABLE II.

Parameter	Value(mm)	Parameter	Value(mm)
W_{Sub}	20	L_{Sub}	25
W_f	3	L_f	10
W	12	L_S	4.47
W_S	8.3	L_g	3
W_P	3	d_S	0.5
R	8	L_r	7.5

TABLE III.

Network Structure	Feed-Forward
Training Algorithm	Levenberg-Marquardt
Performance Algorithm	Mean-Square Error (MSE)
Hidden Layer Structure	[3,5,1]
Learning rate	net.trainParam.lr = 0.05
Performance goal	net.trainParam.goal = 1e-3
Physical parameters	$L_S, W_S,$ and W_d